Scientific Research Publishing

International Journal of Geosciences, 2022, 13, 695-714
https://www.scirp.org/journal/ijg
ISSN Online: 2156-8367
ISSN Print: 2156-8359

Petrography, Geochemistry and Petrogenesis of the Basalt Flow at Al Azraq Al Shamali Area, East Jordan

Ibrahim Ahmad Bany Yaseen[1*], Abd Alkareem Eefan Al Smairan[2]

[1]Department of Earth and Environmental Sciences, Faculty of the Earth and Environmental Sciences, Al-al-Bayt University, Al-Mafraq, Jordan
[2]Directorate of Education for the North Eastern Badia, Ministry of Education, AL-Mafraq, Jordan
Email: *ibanyyaseen@yahoo.com, *ibanyyaseen@aabu.edu.jo, sumeran119@yahoo.com

How to cite this paper: Yaseen, I.A.B. and Al Smairan, A.A.E. (2022) Petrography, Geochemistry and Petrogenesis of the Basalt Flow at Al Azraq Al Shamali Area, East Jordan. *International Journal of Geosciences*, **13**, 695-714.
https://doi.org/10.4236/ijg.2022.138037

Received: June 22, 2022
Accepted: August 28, 2022
Published: August 31, 2022

Abstract

Al Azraq Al Shamali (AZS) basaltic rocks were investigated aiming to understand their mineralogy, petrography and geochemistry features, and to achieve that a total of sixteen representative rock samples were selected for both geochemical and petrographic analysis from several sites in the study area. Petrographic characteristics were analyzed by optical microscopy after preparation thin sections for representative rock samples, which show that all basalt samples have minerals comprising: olivine, plagioclase (labradorite), clinopyroxene (augite), opaque's and some secondary minerals such as Iddingsite, however, the proportions of each mineral vary between samples. Normative mineralogy by using CIPW Norm showed that AZS basalt samples dominated by olivine, Diopside, and nepheline, and AZS basalt can be normatively classified as alkali olivine basalt. Some textures that may be evident on microscopic examination such as porphyritic, glomeroporphyritic, vesicular, intergranular, and ophitic to sub-ophitic texture. X-Ray Fluorescence was used for whole rock major elements analysis (SiO_2, TiO_2, Al_2O_3, Fe_2O_3, MnO, MgO, CaO, Na_2O, K_2O and P_2O_5 in wt%) and trace element (V, Cr, Co, Ni, Rb, Sr, Y, Zr, Nb, Ce, Nd and Ba in ppm). Geochemical analysis reveal that the basalt is alkaline and includes into Sodic series. AZS basalt are produced under-saturated within intraplate continental environment. The normalized trace element diagrams suggest that the AZS product of the asthenosphere part of the mantle at >100 km depth. Furthermore, the data of studied samples suggest that these rocks evolved from a melt formed by low degrees of partial melting. Also the geochemical variation trends of (AZS) basaltic samples supposing that the composition of these basalt have been influenced by fractional crystallization, without clear evidences for crustal con-

tamination.

Keywords

Petrography, Geochemistry, Petrogenesis, Alkali Basalt, Al Azraq Al Shamali Area, Jordan

1. Introduction

Basalts are aphanitic igneous extrusive volcanic rocks formed by the rapid cooling of lava, composed of fine grains of plagioclase, pyroxene, olivine, hornblende and less than 20% quartz [1]. The basalt is the most common rock in the earth's crust; it forms from the melting of the upper mantle and its chemistry closely like the upper mantle's composition. The magma erupt in wide variety of tectonic environments on earth such as mid-ocean ridges, island arcs, back-arc basins, intraplate oceanic islands, large igneous provinces and intra-continental rifts [2]. According to chemical and mineralogical compositions of basalt there are two main types of basalt rocks; tholeiites which are silica saturated-oversaturated and alkali basalts that are silica under saturated. Huge eruption of basalts invariably takes the forms of lava flows, two Hawaiian words are used to describe the two main types of basaltic lava flows are (pahoehoe) lava which is characterized by a smooth or ropy surface and (a'a) lava described by jagged or rough surface [2] [3]. Basalt that forms from magma that extrudes into ocean water forms a type of basalt called "pillow lava" or "pillow basalt".

Basalt in Jordan is a part of the Arabian plateau basalt, which covers a large area from Syria to Yemen through Jordan and Saudi Arabia [4] (**Figure 1**). It comprises one of the world's largest alkaline volcanic provinces named the Arabian Harrat Province, and covers an area of 180.000 km^2 [5]. The volcanism in Harrat Ash Shaam started about 24 million years ago (Miocene to Pleistocene) and continued to recent times with a volcanic hiatus (gab) of several million years between 13 and 7 Ma (a quiescent interlude in volcanic activity) in the northern part of the Harrat Ash Shaam [6]-[13]. Based on K-Ar dating, [6] [14] and [10] have divided the volcanic activity of Jordan into three major episodes: Oligocene to early Miocene (26.23 - 22.17 Ma), middle to late Miocene (13.97 - 8.94 Ma), and late Miocene to Pleistocene (6.95 Ma to <0.15 Ma).

The basalt in Jordan occurs as sporadic small volcanic centers along the eastern side of Dead Sea boundary and as a large area of volcanic field to the northeast of the plate boundary [11]. The N-S striking of Dead Sea Transform (DST) was accompanied by substantial horizontal sinister displacement and by sinisterly fan-like rotation of Arabian plate. These tectonic activities led to opening ways (fissure systems) for the ascent of magmas [15]. The fissure systems trending E-W and NW-SE direction along the eastern margin of the DST, on the large

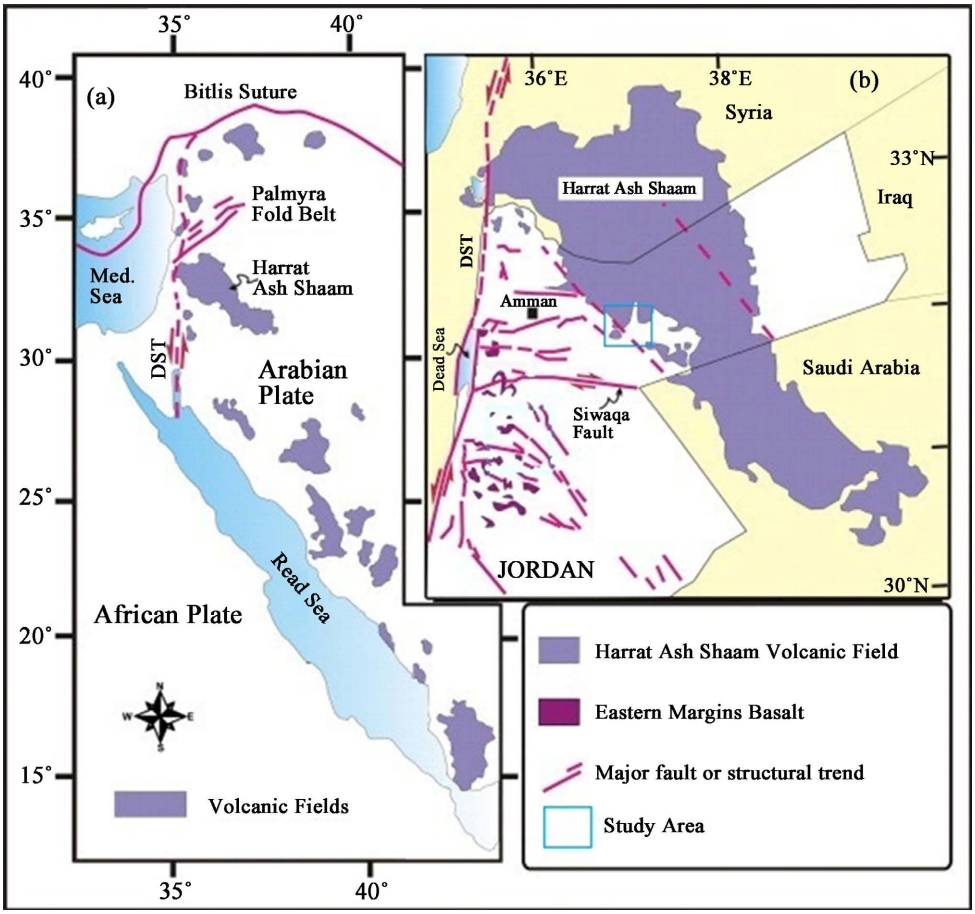

Figure 1. Distribution of intraplate volcanic fields of the Arabian Plate and Location of study area, modified after [4].

basaltic plateau [6]. The Cenozoic basaltic rocks in Jordan are nearly occupy 18% of Jordan area; and they are distributed in three main regions: 1) basalts relating to the DST (e.g. Zara basalt), 2) central Jordan (e.g. El-Lajjoun Basalt), and 3) NE-Jordanian Harrat (with an area 11,400 km^2) which is a part of the largest Harrat Ash Shaam. The central Jordan basalt is found mainly in six places, El-Lajjoun, Jabal Shihan, Tafila, Wadi Dana, Jurf Al-Darawish and Ghor Al-Katar. They occur either as plateau basalts, or as local flows (e.g., Wadi fills) or as individual volcanic bodies (cones, plugs, sills, and dikes) [16]. The southern Jordan basalt is very limited, but there are some studies that have been carried out, such as the study of the origin of the Miocene Mudawwara-Quwayra Basaltic Dike [17]. The study area Al Azraq Al Shamali basalt flow which is a part of Harrat Ash Shaam area, located in the eastern part of Jordan within 36˚47'31" to 36˚51'03" longitudes and 31˚51'36" to 31˚54'35" latitudes. The main objectives of this study evaluate the mineralogy, petrography, and geochemistry features of the basalt flow by using different techniques.

2. Geological Setting

The study area (Al Azraq Al Shamali), situated on the eastern part of Jordan

roughly 75 km east of Amman City. The study area covered by sedimentary and volcanic rocks Figure 2. The sedimentary rocks represented by superficial deposit within quaternary age, exposed in the central part of Al Azraq area. These deposits include alluvial mudflats, fluviatile, colluviums and Wadi sediments [18]. The volcanic rocks are represented with Abed Olivine Phyric Basalt Formation (AOB). These formation (AQB) is one of the three formations of the Safawi group, widespread and dominant in the Al Azraq Al Shamali area, comprises several basaltic flood lava and feeder dike systems. It comprises massive flows up to 10 m thick with a total thickness of up to 100 m, the formation is Late Miocene in age [18].

The study area is located between two NW-SE trending major faults these are 1) Fuluq Fault system (NW-SE) is a normal fault system with downthrown to the southwest and characterized by strike-slip movement; 2) as Sirhan Fault Zone (NW-SE) the As sirhan fault is the western boundary of the sirhan basin, it consists of a series of NW-SE faults; 3) Al Bayda Fault (NW-SE) which represents the border of the main mudflat in the northeastern; 4) al Baqawiyya fault (SW-NE) which may have a horizontal component, it forms the southeastern edge of Qa Al Azraq [19].

3. Sampling and Analytical Techniques

A total of 16 representative rock chip samples were collected from the outcropping of Abed Olivine Basalt Formation (AOB) in eastern Jordan (Figure 2). The

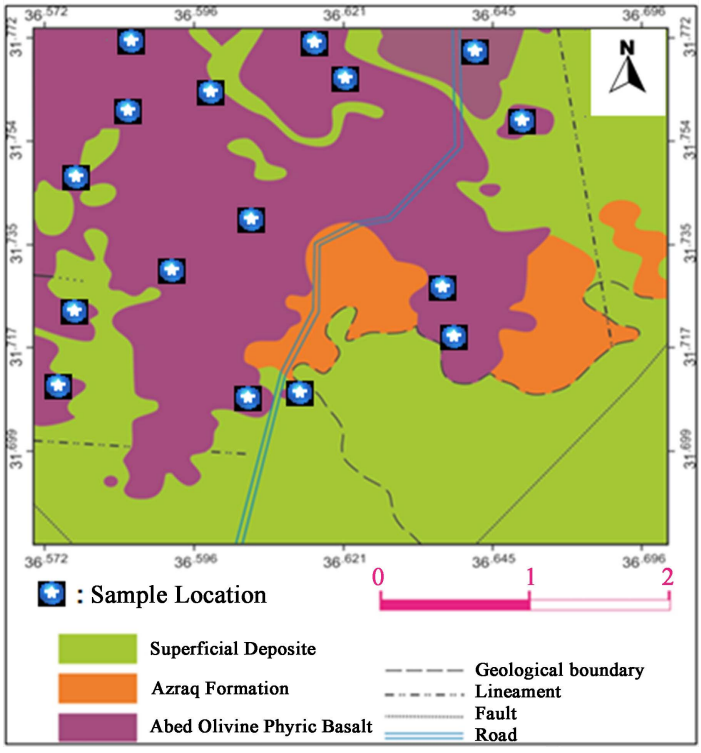

Figure 2. Geological Map of the study area and showing the rock sample locations modified after [20].

samples are crushed and powdered using a stainless steel Jaw Crusher and an Agate Ball Mill machine to obtain a grain size (less than −80μ). The samples were quartered to get a statistically representative (splitter) fraction and powdered using two geochemical techniques at the labs of Al al-Bayt University. The major and trace elements were analyzed on fused glass discs-like pellet (bead) using a pressed pellet using X-Ray Fluorescence Spectrometry (ARL ADVANT'X Intelli Power) model in the laboratories of Jordan Phosphate Mines Company (JPMC) and by Philips XRF (MAGIX PRO PW 2440) model in the laboratories of The Water Environment and Arid Region Research Center Lab at Al al-Bayt University. Using 8.0 gram from each grinded sample and 1.2 grams of grinded cellulose binder were added together on an analytical balance and mixed for approximately one minute. The resulting mixture were put in crucible and putted in oven at 70˚C for 2 hours. The resultant fine powder samples were pressed by press with pressure pumped to (4 tons) for (1 min) in (40 mm) mold (unified) to get the clear disc-like pellet at laboratories of Jordan Phosphate Mines Company. Thin section prepared at the Al al-Bayt University lab, and the photomicrographs of the thin sections were carried out using a LEICA-DMEP Canon camera in the petrography unit at Ministry of Energy and Minerals Resources. The geochemical data processed and pictorially represented by using the computer programs Excel, Igpet 32 and GCD kit and CIPW Norm program for [21].

4. Results and Discussion

4.1. Petrography and Mineralogy

The basaltic rocks samples taken from Al Azraq Al Shamali lava flows are dark, fine-grained to aphanitic rocks with few vesicular samples. The average modal percentage mineral composition of the samples is 60% plagioclase, 15% pyroxene, 13% olivine, 6% opaque minerals (mainly iron oxide), 4% vesicles and 2% secondary minerals such as Iddingsite, calcite and clay. The main common texture of the studied samples was porphyritic, glomeroporphyritic, intergranular, ophitic to sub-ophitic, Radiate, intergranular, seriate, vesicular and amygdaloidal texture.

4.1.1. Plagioclase

Plagioclase crystals are the predominant minerals in thin sections of all samples, forming about 60% of the rock and occur as lath-like shape, subhedral to euhedral tabular shape, and range in size from fine to coarse grain, simple and multiple twining is common. Oscillatory zoning is also noted in some crystals (**Figure 3(a)**). Some crystals displaying inclined extinction. Plagioclase crystals are elongated and occurs with ophitic to sub-ophitic texture enclosed in clinopyroxene crystal and show slight alignment exhibited orientation to olivine and pyroxene crystals. The Ternary Classification Ab-An-Or for feldspars shows that plagioclase minerals of the AZS basalt rocks are plot within the labradorite field (**Figure 4(a)**).

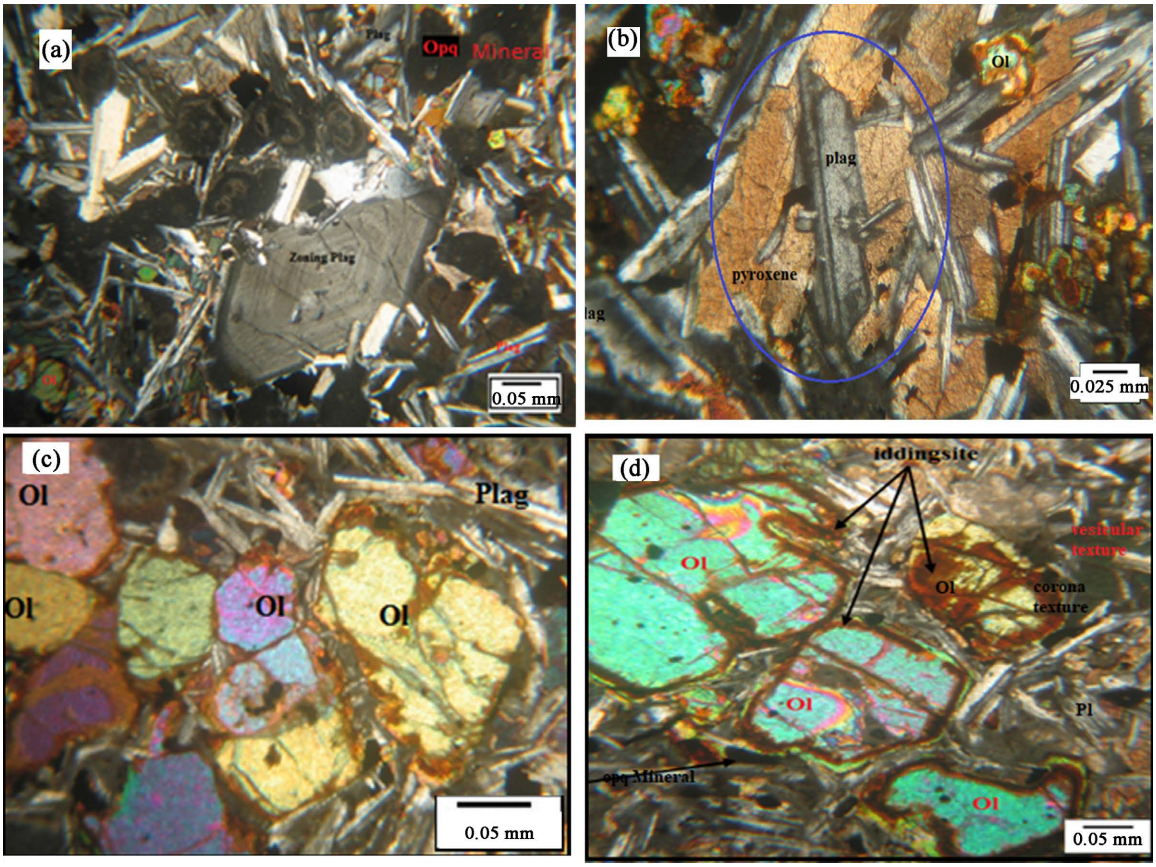

Figure 3. Photomicrograph showing (a) Oscillatory zoning of plagioclase (XPL), magnification, 4×. sample 8. (b) Ophitic texture, where plagioclase laths are completely enclosed by pyroxene mineral (XPL), magnification 10×, sample No. 13. (c) Glomeroporphyritic texture, where the Phenocrysts (Plagioclase and olivine) are found to occur as clusters of crystals (XPL magnification, 4×, Sample No. 13. (d) Corona and Iddingsite texture (XPL), magnification 4×, Sample No.9. Where 4× = 0.1 mm, 10× = 0.25 mm, (Ol: Olivine; Plag: Plagioclase; Opq: Opaque minerals).

4.1.2. Pyroxene

Pyroxene occurs as colorless to grayish brown in color with anhedral crystals, comprising about 15% of the rock, the crystals have sizes between 0.3 to 0.5 mm, and they show perfect two set of cleavage intersect at ~90˚ in the cross-section. The clinopyroxene intersected with plagioclase crystals to form ophitic to sub-ophitic textures (**Figure 3(b)**). The classification scheme of Morimoto (1988), clinopyroxene is fall in the augite field near the Diopside/Hedenbergite boundary (**Figure 4(b)**). The clinopyroxene intersected with plagioclase crystals to form ophitic to sub-ophitic textures

4.1.3. Olivine

The olivine Phenocrysts occurs as single or clustered subhedral to anhedral crystals, and forming ~13% of the rock, high relief and ranging between 0.02 and 0.75 mm in diameter displaying seriate texture. Moreover, when plagioclase and olivine Phenocrysts are found to occur as clusters of crystals exhibit glomeroporphyritic texture or aggregated within the intergranular spaces between plagioclase laths (**Figure 3(c)**). Olivine high degree of alteration to Iddingsite. The

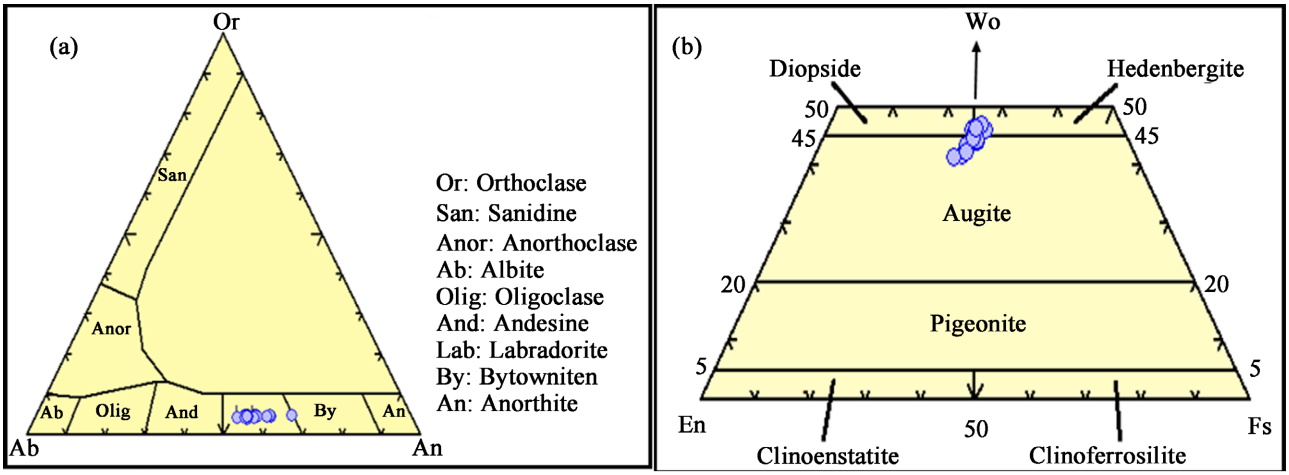

Figure 4. (a) Ab-An-Or ternary plot for plagioclase compositions of AZS samples, all the ample plotted within Labradorite field, modified after [22]. (b) Pyroxene Classification from the AZS basalts, the sample plotted within augite field, modified after [23]. Wo: Wollastonite; En: Enstatite; Fs: Ferrosilite.

crystals are fractured slightly to moderately, Iddingtization are also noted particularly along the edge (rim) and fractures of the crystals, some crystals were partially to completely pseudo morphed to brown Iddingsite and corona texture (**Figure 3(d)**).

4.1.4. Secondary Minerals

Secondary minerals resulting from introduced or substituted during the processes of alteration, metamorphism, or weathering that changes in the primary or original mineral constituents of the rock [1]. The microscopic investigations of samples show that these processes include alteration of olivine to produced Iddingsite. Opaque minerals (mainly iron oxide) were commonly found in thin sections, range in size from 0.03 mm to 0.05 mm, forming about 6% of the rock, opaque minerals common with anhedral shape, most of them occurred as hematite dispersed between plagioclase, pyroxene and olivine crystals (**Figure 3(c)** and **Figure 3(d)**) calcite and clay minerals then we called the texture amygdaloidal, the long axis of these vesicles ranges from 0.05 to 0.35 mm and formed about 4% of the rock.

4.2. Geochemistry

4.2.1. Major Oxides

Al Azraq Al Shamali (AZS) basalt have been investigated by Sixteen rock samples, were analyzed the major oxides (SiO_2, TiO_2, Al_2O_3, Fe_2O_3, MnO, MgO, CaO, Na_2O, K_2O and P_2O_5 (wt%)) and trace elements V, Cr, Co, Ni, Rb, Sr, Y, Zr, Nb, Ce, Nd and Ba (ppm) is listed in **Table 1.** The content of SiO_2 varies from 44.4 wt% to 48.9 wt% with an average of 46.4 wt%, which is within the average value reported by several authors for alkali basalt and basanite [24] [16] [11] [25] [26], and it can be classified as basalt to Trachy basalt using the Total Alkalis Vs. Silica classification scheme [27] and [28] (**Figure 5(a)** and **Figure 5(b)**). The total alkali-silica diagram, with the [29] show that AZS basalt samples

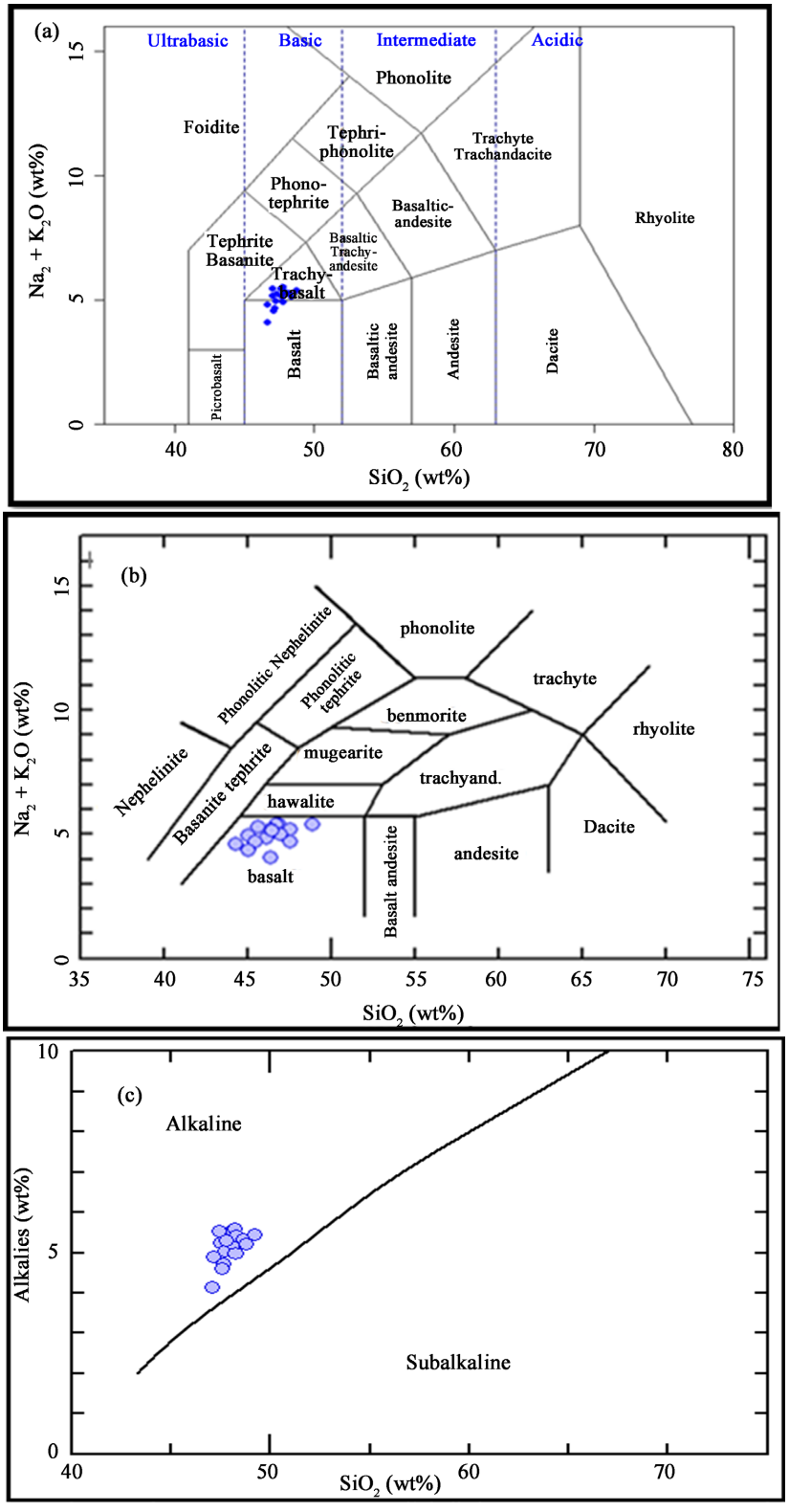

Figure 5. (a) TAS diagram, after (Le Bas *et al.* 1986), shows the AZS sample located within basaltic to Trachy basalt field. (b) SiO_2 vs. $Na_2O + K_2O$ (TAS) diagram after [28], showing the classification of volcanic rocks from AZS. All the rock samples were plotted within basalt field. (c) The total alkali-silica diagram, with the [29] boundary line which show that AZS basalt samples dominantly plot within alkaline field.

dominantly plot within alkaline field (Figure 5(c)). These results have been documented by many authors such as [26] [30] [31] [32] [33] [34]. According to [35], diagram for the alkali series into sodium, potassium and potassium-rich series, the AZS basalts samples were found to belong to the sodic series (Figure 6). The variation ranges of other major elements oxides such as Al_2O_3 content ranges from 16.7 wt% to 19.6 wt% with average of 18.2 wt%, Fe_2O_3 varies between 9.9 wt% and 10.6 wt% with average of 10.2 wt%. MnO range between 0.13 and 0.15 wt% with average of 0.14 wt%. MgO range between 4.1 wt% and 6.2 wt% with average of 4.9 wt% CaO range between 9.9 wt% and 12.9 wt% with average of 10.9 wt%. Na_2O range between 3.3 wt% and 4.7 wt% with average of 4.2 wt%. K_2O range between 0.6 wt% and 0.8 wt% with average of 0.7 wt% and P_2O_5 between 0.3 wt% and 0.9 wt% with average of 0.4 wt%. The Mg number (Mg#), defined as the molecular proportion of $Mg^{2+}/(Mg^{2+} + Fe^{2+})$ and usually used as a petrogenetic indicator for magma fractionation and its primitive volcanic rocks [36] [30]. The Mg# varies from 62 to 70 with average of 65 (Table 1).

The major elements concentrations were used to calculate the CIPW norm (Table 1). The Normative albite has higher concentrations than anorthite, which indicates the alkaline in nature of these rocks. Diopside and Nepheline are present in the AZS rock samples and low percent of apatite, perovskite and ilmenite respectively. Based on CIPW normative calculations and the classification scheme of alkali basalts proposed by [37], the studied samples are plotted in the alkali olivine basalt field (Figure 7).

4.2.1. Trace Elements

The AZS basalt samples high concentration of Ni and Cr, range between 147 to 232 with average 192 ppm, Cr range between 432 to 590 with average 505 ppm, it is may indicate for derivation of parental magmas from a peridotite mantle

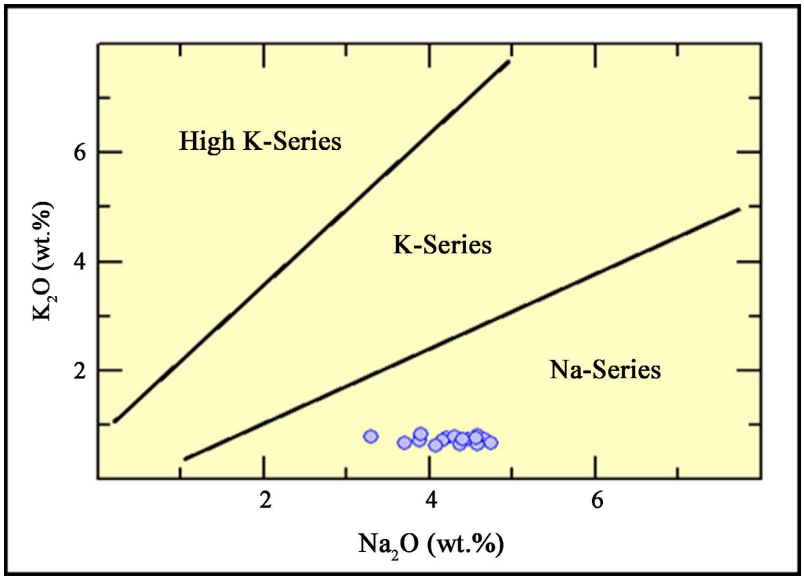

Figure 6. K_2O vs. Na_2O diagram showing the study samples plotted within Sodic Series, after [38].

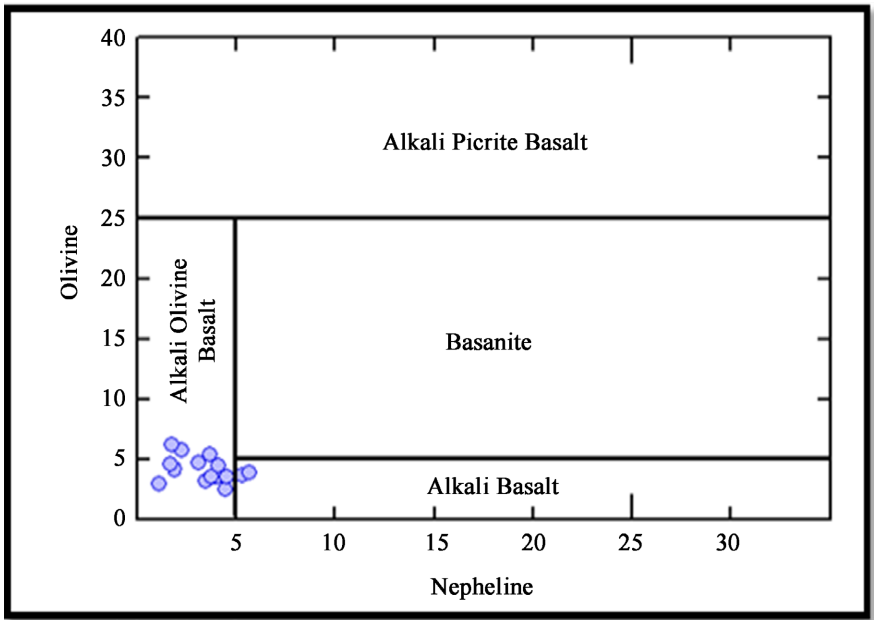

Figure 7. Plots of normative olivine (wt%) against normative nepheline (wt%) compositions of AZS alkali basalt, after [39].

Table 1. Chemical analysis of the AZS basaltic sample studied.

Sample No.	AZS 1	AZS 2	AZS 3	AZS 4	AZS 5	AZS 6	AZS 7	AZS 8
SiO_2 wt%	46.4	46.04	46.9	46.2	46.6	46.9	46.7	46.4
TiO_2	1.7	1.9	1.9	1.8	1.7	1.7	1.8	1.9
Al_2O_3	16.7	17.4	18.2	17.8	19.6	18.1	18.2	18.5
Fe_2O_3	10.5	10.4	10.3	10.5	10.3	10.1	10	9.9
MnO	0.15	0.14	0.14	0.14	0.14	0.14	0.14	0.13
MgO	4.95	4.8	4.97	5.3	4.1	4.8	4.6	4.1
CaO	11.7	11.8	10.4	10.9	11.8	11.2	10.6	10.6
Na_2O	3.9	4.2	4.6	4.2	3.9	4.3	4.7	4.5
K_2O	0.71	0.76	0.8	0.7	0.81	0.8	0.73	0.73
P_2O_5	0.35	0.33	0.34	0.3	0.9	0.4	0.34	0.33
Total	97.06	97.77	98.55	97.84	99.85	98.44	97.81	97.09
LOI	2.94	2.23	1.45	2.16	0.15	1.56	2.19	2.91
Mg#	65	64	66	67	62	65	63	63
Trace Elements (ppm)								
V	180	185	193	196	195	190	202	199
Cr	432	458	454	529	566	437	457	470
Ni	171	197	172	191	187	169	147	164
Sr	514	283	749	2530	793	574	514	544
Y	12	17	15	11	15	17	14	15

Continued

Zr	123	40	122	143	137	134	120	116
Nb	13	18	14	8.4	17	13	17	13
Zr/Nb	9.5	2.2	8.7	17	8	10.3	7.1	9
Nb/Y	1.1	1.1	0.9	0.8	1.1	0.8	1.2	0.9
Zr/Y	10.3	2.4	8.1	13	9.1	7.9	8.6	7.7
CIPW-Norms wt%)								
Or	4.19	4.47	4.7	4.11	4.77	4.5	4.31	4.34
Ab	24.62	28.14	31.13	29.55	32.41	29.61	31.09	31.42
An	25.98	26.33	26.64	27.77	33.7	27.88	26.66	28.13
Di	19.05	14.8	13.18	14.25	10.7	15.42	13.7	12.68
Ne	4.45	4.04	4.14	3.08	5.36	3.7	4.57	3.45
Ol	2.45	3.57	4.4	4.68	3.68	3.38	3.56	3.12
Hm	10.48	10.4	10.31	10.46	10.28	10.06	10.01	9.86
Ap	0.8	0.76	0.79	0.7	1.97	0.83	0.78	0.77
Pf	2.71	2.96	2.93	2.86	2.69	2.69	2.88	2.95
Il	0.33	0.3	0.29	0.3	0.3	0.3	0.3	0.28
Sample No.	**AZS 9**	**AZS 10**	**AZS 11**	**AZS 12**	**AZS 13**	**AZS 14**	**AZS 15**	**AZS 16**
SiO_2 wt%	47.6	48.9	45.4	47	46.5	45.7	46.4	46.1
TiO_2	1.4	1.6	1.5	1.5	1.8	1.8	1.5	1.7
Al_2O_3	18.9	18.2	18	18.9	18.2	18.1	18.7	17.9
Fe_2O_3	9.9	10.1	10.3	10.9	10.4	10.3	10.6	10.4
MnO	0.14	0.14	0.15	0.14	0.14	0.14	0.15	0.14
MgO	4.6	5.4	4.6	4.4	5.4	4.8	4.8	6.2
CaO	10.7	9.9	10.2	10	10.4	10.7	12.9	10.7
Na_2O	4.6	4.7	4.1	4.4	4.4	4.6	3.3	3.7
K_2O	0.6	0.7	0.6	0.6	0.7	0.7	0.8	0.7
P_2O_5	0.3	0.3	0.3	0.3	0.3	0.3	0.6	0.3
Total	98.74	99.94	95.15	98.14	98.24	97.14	99.75	97.84
LOI	1.26	0.06	4.85	1.86	1.76	2.86	0.25	2.16
Mg#	65	68	64	63	67	65	64	69
Trace Elements (ppm)								
V	177	168	190	183	190	193	176	189
Cr	495	504	478	476	590	588	588	564
Ni	198	211	191	196	205	227	218	232
Sr	1280	518	730	643	618	616	779	547

Continued

Y	17	13	14	17	18	15	17	14
Zr	115	110	120	115	120	123	127	121
Nb	9.1	13	8.4	9.8	12	13	12	14
Zr/Nb	12.6	8.5	14.3	11.7	10	9.5	10.6	8.6
Nb/Y	0.5	1	0.6	0.6	0.7	0.9	0.7	1
Zr/Y	6.8	8.5	8.6	6.8	6.7	8.2	7.5	8.6
CIPW-Norms (wt%)								
Or	3.71	3.85	3.66	3.72	4.31	4.37	4.56	3.89
Ab	3.71	3.85	3.66	3.72	4.31	4.37	4.56	3.89
An	31.85	36.06	30.98	33.95	30.5	28.21	25.81	28.19
Di	29.14	27.63	29.11	30.29	27.81	26.72	33.9	27.64
Ne	13.65	11.34	11.95	10.02	12.44	14.15	16.85	14.17
Ol	3.77	2.23	1.89	1.67	3.7	5.68	1.14	1.73
Hm	3.54	5.73	4.15	4.51	5.35	3.85	2.89	6.2
Ap	9.92	10.07	10.26	9.93	10.44	10.28	10.55	10.36
Pf	0.66	0.65	0.61	0.66	0.75	0.77	1.3	0.74
Il	2.15	2.53	2.24	2.25	2.79	2.86	2.21	2.58

An: Anorthite; Or: Orthoclase; Ol: Olivine; Ab: Albite; Di: Diopside; Ap: Apatite; Il: Ilmenite; He: Hematite; Pf: perovskite; Ne: Nepheline.

source [40]. The high content of Cr and Ni indicated by the parental magma had been derived through partial melting of peridotite mantle source, and suggested that presence of olivine and clinopyroxene fractions in the AZS [3] [11] [26] [40]. The concentration of Sr and Zr, in the AZS rock sample study had relatively high contents. The Sr ranging between 283 to 2530 ppm with average of 764 ppm, Zr content between 40 to 143 ppm with average of 117 ppm, (**Table 1**). The Sr^{+2} is substitute for Ca in plagioclase minerals (Anorthite $CaAl_2Si_2O_8$) and lesser extent was found in K-feldspar. Zr is found in accessory minerals such as Zirconium ($ZrSiO_4$) [41] [42]. The Rare Earth Elements (REE) includes Nb and Y content ranging between 8 to 18 ppm with average 13, Nb range between 11 to 15 with average 15 ppm respectively. The REE were replacement of Ca^{+2} in accessory minerals such as Apatite $Ca_5(PO_4)$ (OH, F, Cl) and Titanite ($CaTiSiO_5$). Niobium (Nb^{5+}) does not substitute for major elements because of its high charge, but it may substitute for titanium due to their similar ionic radii and valence state [42]. Vanadium concentration range between 168 to 202 with average 187 ppm. Vanadium and Titanium has a comparable behaviour in melting and crystallization processes, those elements provide a useful signal for of the fractionation of Fe-Ti oxides (such as ilmenite) [40]. The average ratio between Zr/Nb, Nb/Y and Zr/Y are 9.85, 0.86 and 8.0 respectively. These ratios were documented

and reported by [32] [43] for the intercontinental alkali basalt.

5. Petrogenesis

The chemical analysis of major and trace elements for AZS basaltic rock samples study was used to construct the discriminate diagrams, which help to classification, nomenclature and interpretation of the tectonic setting of the AZS basalt. Ti-V diagram after [44] dependent on a variable valence state of vanadium and ranges in titanium abundances to delineate mid-ocean ridge, Ocean Island and volcanic-arc basalt. The study samples fall within the alkaline field (**Figure 8**). The ternary diagram for Ti-Zr-Y, after [45], the studied samples fall within plate basalt field **Figure 9(a)**. The Zr-Nb-Y diagram after [46], shows all the study samples plotted and fall within the fields A and B, these indicating an intraplate tectonic setting (**Figure 9(b)**). The MnO-TiO_2-P_2O_5 diagram after) [47], all the studied samples are located within the (OIA) field, (**Figure 9(c)**).

The spider diagrams for Rock Primordial mantle are used to study for AZS basaltic rock samples (AZS). The study samples show enrichments with peaks at Nb and Sr, and depletions for the high field strength (HFS) elements of Zr, Ce and Ti, in addition to a little variation in Y contents. The negative (K) anomalies are obviously a common feature of Si-under saturated basic magmas and indicate for a smaller degrees of partial melting, also the strong positive Sr anomalies reflects the higher content of (Sr) element in the samples which is a feature inherited from the mantle source [48]. The presence of negative (P) anomaly indicates a crystallization of apatite [49]. The negative anomalies of HFS elements (Zr, Ce, Ti and Y) in primitive mantle-normalized diagrams (**Figure 10**), are incompatible with a fundamental involvement of continental crust in the genesis of AZS basaltic rocks (Doroozi *et al.* 2018). A slightly positive Nb peak is a

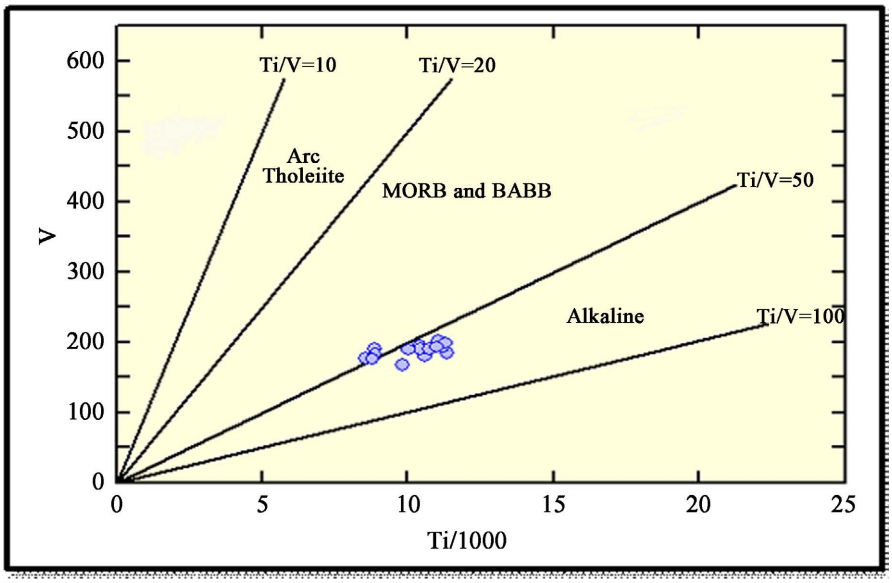

Figure 8. Ti/1000 vs. V discrimination diagram after [44], AZS basalt samples. Within Alkaline field, MORB: mid-ocean ridge basalt; BABB: back-arc basin basalt.

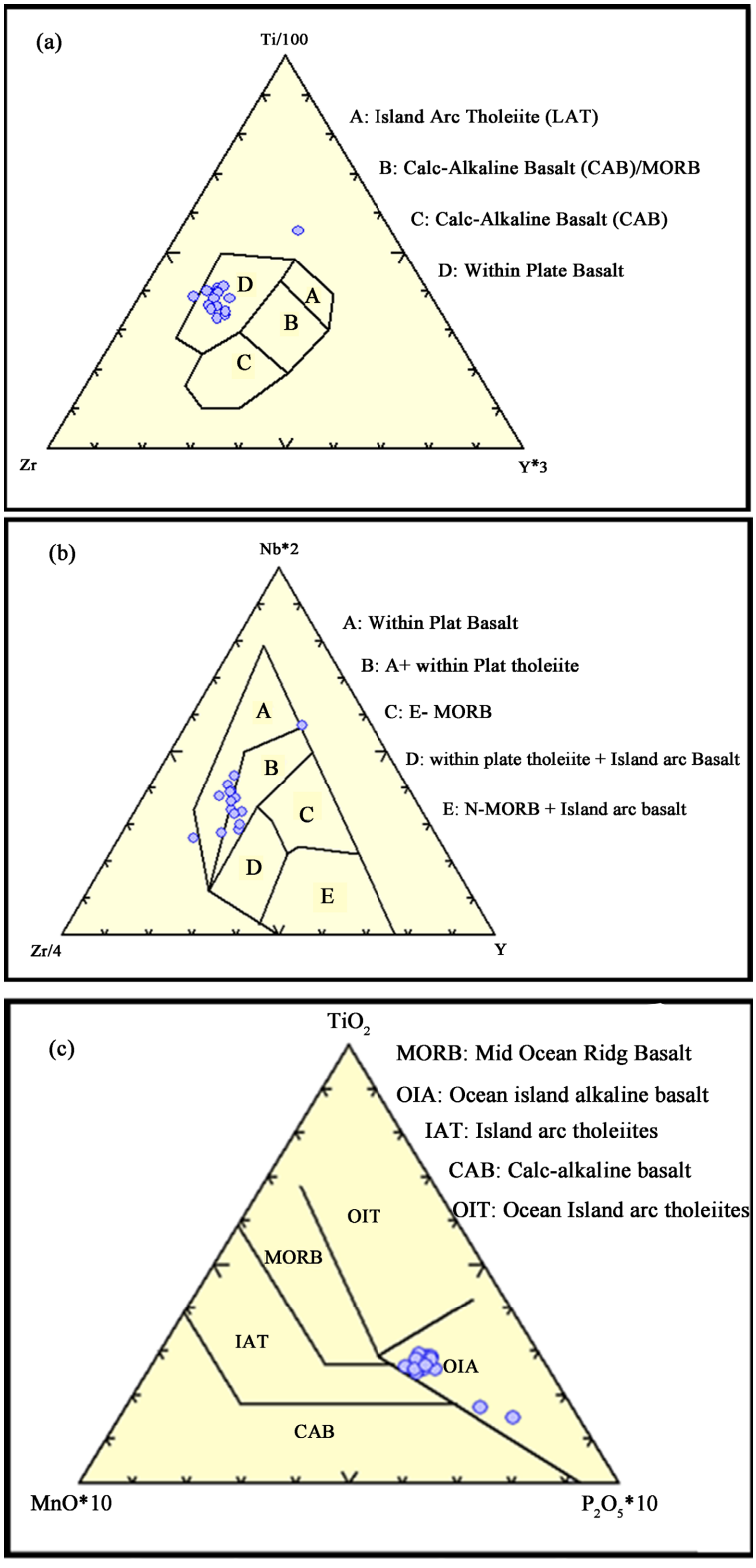

Figure 9. (a) Ti-Zr-Y diagram of after (Pearce and Cann, 1973) for the AZS basalt samples, shows the studied samples fall in the (D)-within plate basalt field; (b) the Nb –Zr– Y diagram after [46] for the AZS basaltic samples, shows the studied samples within A and B fields; (c) TiO_2-MnO-P_2O_5 diagram after [47], for AZS basaltic samples plotted within OIT: ocean island tholeiites field.

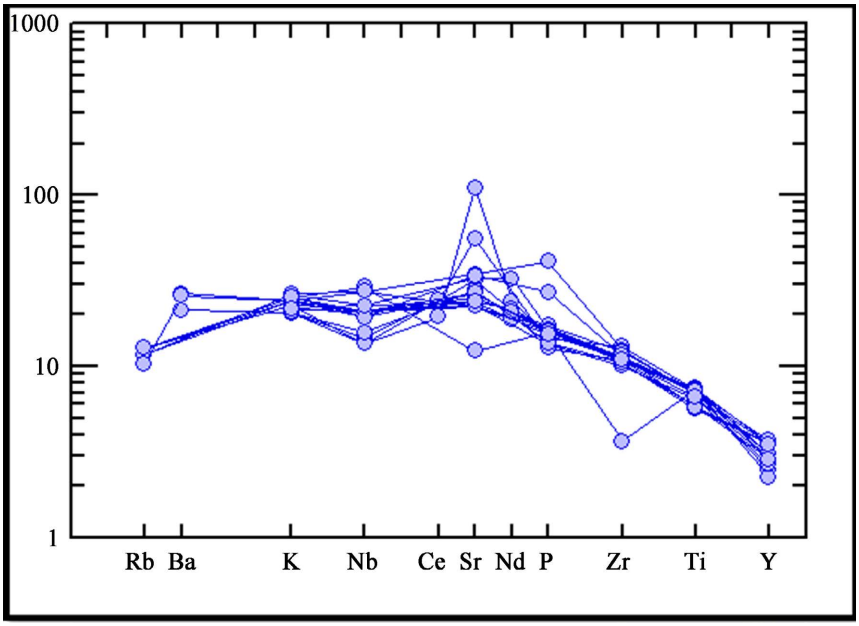

Figure 10. Primitive mantle-normalized incompatible trace element abundance patterns of the AZS basaltic rocks, after [54].

distinctive feature of continental and oceanic alkali basalts [50], and considered a good indicator that the AZS is a product of the asthenosphere part of the mantle rather than the lithosphere [16]. It can be noticed, that the positive Ba and Sr anomalies and slight negative Zr and Ti anomalies reflect that the general multi-element distribution patterns of the AZS alkali basalt samples shows an OIB-like feature [51] [52], except the trace element Sr, which has relatively higher contents (average ~ 764 ppm) than those of normal OIB (average ~ 660 ppm) [53].

The binary diagram for Zr-Nb plot after Bakhsh, 2015, **Figure 11** explain the geochemical characteristics and petrogenetic studies of the AZS basalt have indicated that the magmas initially originated by a low partial melting (~ 10%) and the peridotite precursor was most probably spinel lherzolite rather than garnet.

6. Conclusions

The following present of the study area are:

1) All the samples mainly contain olivine, pyroxene, plagioclase and opaque with secondary mineral phases such as Iddingsite which is a result of the alteration processes of olivine.

2) Many types of textures have been observed in AZS samples such as porphyritic, glomeroporphyritic, vesicular, intergranular, radiate, and ophitic to sub ophitic texture.

3) Petrographically, we can classify AZS basalt samples as Alkali-olivine basalt.

4) Normative mineralogy by using CIPW norm showed that AZS basalt samples dominated by anorthite, albite, olivine, orthoclase, Diopside, hematite, nepheline, olivine and low percent of apatite, perovskite and ilmenite.

5) The chemical classification of AZS basalt samples classified as alkaline basalt

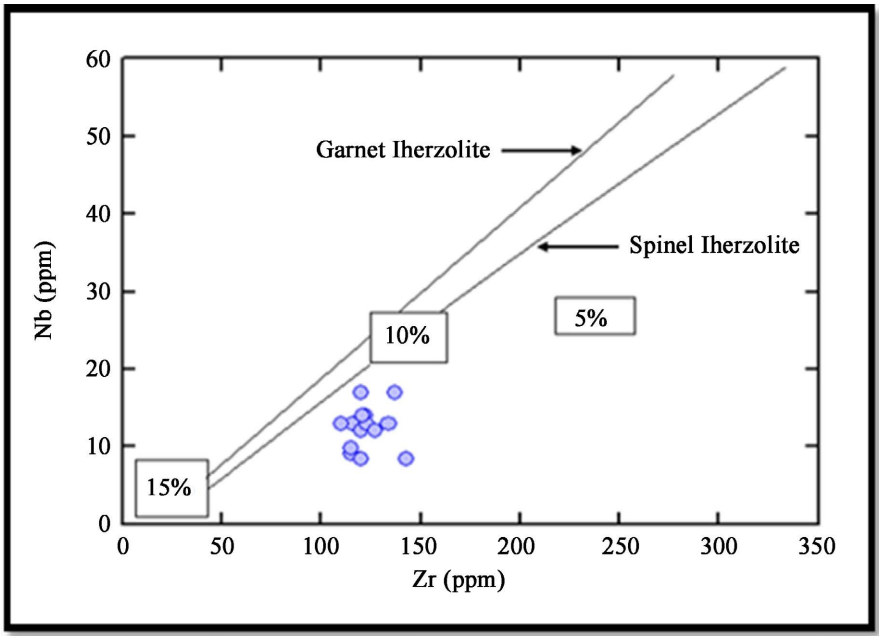

Figure 11. Zr-Nb plot of AZS basalt samples, show that the peridotite precursor was most probably spinel lherzolite rather than garnet, with a small degree of melting, modified after [54].

and belongs to sodic series.

6) The tectonic setting for the discrimination diagram showed that the AZS samples are situated within plate basalt field.

7) The AZS basalts were produced by primary magmas, were mainly resulted by low degrees of partial melting of garnet-bearing peridotite within the asthenosphere at >I00 km depth, and underwent fractional crystallization of olivine, pyroxene and the plagioclase in the latest stage.

8) The geochemical characteristics and petrogenetic studies of the AZS basalt provide no clear evidence for crustal contamination being a major influence on these rocks.

9) The normalized trace elements spider diagrams (Primitive mantle) of AZS basalt suggest that the basalt is derivation from a depleted mantle source (precisely from asthenosphere part of the mantle).

Acknowledgements

The author is thankful to the laboratory of the University of Al al-Bayt University, Faculty of the Earth and Environmental Sciences for the geochemical and thin section preparation samples. Thanks to the Water Environment and Arid Region Research Center Labs at Al al-Bayt University, and Jordan Phosphate Mines Company (JPMC) for determine and analysis of the major and trace elements using X-Ray Fluorescence Spectrometry.

Conflicts of Interest

The authors declare no conflicts of interest regarding the publication of this paper.

References

[1] Haldar, S.K. and Tišljar, J. (2014) Introduction to Mineralogy and Petrology. Elsevier, Amsterdam, 338 p. https://doi.org/10.1016/C2012-0-03337-6

[2] Gill, R. (2010) Igneous Rocks and Processes: A Practical Guide. Wiley-Blackwell, Oxford, 428 p.

[3] Winter, J.D. (2014) Principles of Igneous and Metamorphic Petrology: Pearson New International Edition (2e). Pearson Education, USA, 738 p.

[4] Ibrahim, K.M., Moh'd, B.K., Masri, A.I., Al-Taj, M.M., Musleh, S.M. and Alzughoul, K.A. (2014) Volcano Tectonic Evolution of Central Jordan: Evidence from the Shihan Volcano. *Journal of African Earth Sciences*, **100**, 541-553. https://doi.org/10.1016/j.jafrearsci.2014.07.021

[5] El-Akhal, H. (2004) Contribution to the Petrography, Geochemistry, and Tectonic Setting of the Basalt Flows of the Umm-Qais Plateau, North Jordan. *Geological Bulletin of Turkey*, **47**, 1-10.

[6] Barberi, F., Capaldi, P., Gasperihi, G., Marinelli, G., Santacroce, R., Treuil, M. and Varet, J. (1979) Recent Basaltic Volcanism of Jordan and Its Implication on the Geodynamic History of the Dead Sea Shear Zone. In: International Symposium Geodynamic Evolution of the Afro-Arabian Rift System, Academia Nazionale Dei Lincei 47, Rome, 667-683

[7] Guba, I. and Mustafa, H. (1988) Structural Control of Young Basaltic Fissure Eruption in the Plateau Basalt Area of the Arabian Plate, Northeastern Jordan. *Journal of Volcanology and Geothermal Research*, **35**, 319-334. https://doi.org/10.1016/0377-0273(88)90026-1

[8] Mor, D. (1993) A Time-Table for the Levant Volcanic Province, According to K-Ar Dating in the Golan Heights, Israel. *Journal of African Earth Sciences*, **16**, 223-234. https://doi.org/10.1016/0899-5362(93)90044-Q

[9] Sharkov, E.V., Chernyshev, I.V., Devyatkin, E.V., Dodonov, A.E., Ivanenko, V.V., Karpenko, M.I., Leonov, Yu.G., Novikov, V.M., Hanna, S and Khatib, K. (1994) Geochronology of Late Cenozoic Basalts in Western Syria. *Petrology*, **2**, 439-448.

[10] Illani, S., Harlavan, Y., Tarawneh, K., Rabba', I., Weinberger, R., Ibrahim, K. Peltz, S. and Steinitz, G. (2001) New K-Ar Ages of Basalts from the Harrat Ash Shaam Volcanic Field in Jordan: Implications for the Span and Duration of the Upper Mantle Upwelling Beneath the Western Arabian Plate. *Geology*, **29**, 171-174. https://doi.org/10.1130/0091-7613(2001)029<0171:NKAAOB>2.0.CO;2

[11] Shaw, J., Baker, J., Menzies, M., Thirlwall, M. and Ibrahim, K.M. (2003) Petrogenesis of Largest Intraplate Volcanic Field on the Arabian Plate (Jordan): A Mixed Lithosphere-Asthenosphere Source Activated by Lithospheric Extension. *Journal of Petrology*, **44**, 1657-1679. https://doi.org/10.1093/petrology/egg052

[12] Weinstein, Y., Navon, O., Altherr, R and Stein, M. (2006). The Role of Lithospheric Mantle Heterogeneity in the Generation of Plio-Pleistocene Alkali Basaltic Suites from NW Harrat Ash Shaam (Israel). *Journal of Petrology*, **47**, 1017-1050. https://doi.org/10.1093/petrology/egl003

[13] Al-Kwatil, M.A., Gillot, P.Y., Zeyen, H., Hildenbrand, A. and Al Gharib, I. (2012). Volcano-Tectonic Evolution of the Northern Part of the Arabian Plate in the Light of New K-Ar Ages and Remote Sensing: Harrat Ash Shaam Volcanic Province (Syria). *Tectonophysics*, **32**, 192-207. https://doi.org/10.1016/j.tecto.2012.09.017

[14] Duffield, W.A., McKee, E.H., El Salem, F. and Teimeh, T. (1988) K-Ar Ages, Chemical Composition and Geothermal Significance of Cenozoic Basalt Near the Jordan

Rift. *Geothermics*, **17**, 635-644. https://doi.org/10.1016/0375-6505(88)90048-X

[15] Fediuk, F. and Al-Fugha, H. (1999) Dead Sea Region: Fault-Controlled Chemistry of Cenozoic Volcanic. *GEOLINES* (*Praha*), **9**, 29-34.

[16] El-Hasan, T. and Al-Malabeh, A. (2008). Geochemistry, Mineralogy and Petrogenesis of El Lajjoun Pleistocene Alkali Basalt of Central Jordan. *Jordan Journal of Earth and Environmental Sciences*, **1**, 53-62.

[17] Alnawafleh, H., Tarawneh, K., Ibrahim, K., Zghoul, K., Titi, A., Rawashdeh, R., Moumani, K. and Masri, A. (2015). Characterization and Origin of the Miocene Mudawwara-Quwayra Basaltic Dike, Southern Jordan. *International Journal of Geosciences*, **6**, 869-881. https://doi.org/10.4236/ijg.2015.68071

[18] Ibrahim, K., Rabba, I. and Tarawneh, K, (2001). Geological and Mineral Occurrences Map of the Northern Badia Region, Jordan. Scale 1:250.000. Natural Resources Authority (NRA), Geology Directorate, Amman, Jordan.

[19] Ibrahim, K.M. (1996) The Regional Geology of Al-Azraq Area Map Sheet No. 3553I. Bulletin No. 36, Natural Resources Authority, Geological Mapping Division, Amman.

[20] Ibrahim, K.M. (1993) Geological Map of Al Azraq Area, Map Sheet No. 35531. Natural Resources Authority (NRA), Geology Directorate, Amman.

[21] Hollocher, K. (2004) CIPW Norm Calculation Program. Geology Department, Union College, Schenectady.

[22] Yazdi, A., Ashja-Ardalan, A., Emami, M.-H., Dabiri, R. and Foudazi, M, (2017) Chemistry of Minerals and Geothermobarometry of Volcanic Rocks in the Region Located in Southeast of Bam, Kerman Province. *Open Journal of Geology*, **7**, 1644-1653. https://doi.org/10.4236/ojg.2017.711110

[23] Morimoto, N. (1988). Nomenclature of Pyroxenes. *Mineralogical Magazine*, **52**, 535-550. https://doi.org/10.1180/minmag.1988.052.367.15

[24] Ibrahim, K.M. and Al-Malabeh, A. (2006) Geochemistry and Volcanic Features of Harrat El Fahda: A Young Volcanic Field in Northwest Arabia, Jordan. *Journal of Asian Earth Sciences*, **27**, 147-154. https://doi.org/10.1016/j.jseaes.2005.01.009

[25] Al-Malabeh, A. (2009) Cryptic Mantle Metasomatism: Evidences from Spinel Lherzolite Xenoliths/Al-Harida Volcano in Harrat Al-Shaam, Jordan. *American Journal of Applied Sciences*, **6**, 2085-2092. https://doi.org/10.3844/ajassp.2009.2085.2092

[26] Al-Fugha, H. and Yaseen, B. (2019) Petrography, Geochemistry and Petrogensis of Pleistocene Basaltic Flow from Northwest Atarous Area, Central Jordan. *International Journal of Geosciences*, **10**, 613-631. https://doi.org/10.4236/ijg.2019.106035

[27] Le Maitre, R.W., Bateman, p., Dudek, A., Keller, J., Lameyre Le Bas, M.J., Sabine, p.A., Schmid, R., Sorensen, H., Streckeisen, A., Woolley, A.R. and Zanettin, B. (1989) A Classification of Igneous Rocks and Glossary of Terms. Blackwell, Oxford.

[28] Cox, K.G., Bell, J.D. and Pankhurst, R.J. (1979) The Interpretation of Igneous Rocks. Springer, London, 450 p. https://doi.org/10.1007/978-94-017-3373-1

[29] Irvine, T.N. and Baragar, W.R.A. (1971) A Guide to the Chemical Classification of the Common Volcanic Rocks. *Canadian Journal of Earth Sciences*, **8**, 523-548. https://doi.org/10.1139/e71-055

[30] Bany Yaseen, I.A.A. (2014) Contribution to the Petrography, Geochemisty, and Petrogenesis of Zarqa-Ma'in Pleistocene Alkali Olivine Basalt Flow of Central Jordan. *International Journal of Geosciences*, **5**, 657-672. https://doi.org/10.4236/ijg.2014.56059

[31] Bany Yaseen, I.A.A. (2016) Petrography, Geochemistry and Petrogensis of Basal

Flow from Ar-Rabba Area, Central Jordan. *International Journal of Geosciences*, **7**, 378-396https://doi.org/10.4236/ijg.2016.73030

[32] Bany Yaseen, I.A.A. and Abidrabbu, A.Y. (2016) Mineralogy, Petrology and Geochemistry of the Basalt Flows at Ash-Shun Ash-Shamaliyya Area, North West Jordan. Science Publishing Group, New York, 82-95.

[33] Al Smadi, A., Al-Malabeh, A. and Odat, S. (2018) Characterization and Origin of Selected Basaltic Outcrops in Harrat Irbid (HI), Northern Jordan. *Jordan Journal of Earth and Environmental Sciences*, **9**, 185-196.

[34] Nawasreh, A. (2022) Mineralogical and Geochemical Investigation of the Basaltic Rocks along Kharrouba Fault at Qasr Al Hallabat Area. MSC Thesis, Faculty of Earth and Environmental Sciences, Al al-Bayt University Jordan, Al-Mafraq.

[35] Middlemost, E.A.K. (1975) The Basalt Clan. *Earth Science Reviews*, **11**, 337-364. https://doi.org/10.1016/0012-8252(75)90039-2

[36] Bany Yaseen, I.A., Al-Hawari, Z. and Diabat, A.A. (2010) Petrology, Geochemistry, Petrogenesis and Reactivation of Volcanic Tuffs at Dair El-Kahif Area, NE-Jordan. *Jordan Journal of Civil Engineering*, **4**, 336-350. https://doi.org/10.3319/TAO.2010.06.28.01(TT)

[37] Chih, C.S. (1988) The Study of Cenozoic Basalts and the Upper Mantle Beneath Eastern China (Attachment: Kimberlites). China Geosciences University Press, Wuhan, 277 p. (in Chinese)

[38] Ho, K.S., Liu, Y., Chen, J.C., You, C.F. and Yang, H.J. (2011) Geochemical Characteristics of Cenozoic Jining Basalts of the Western North China Craton: Evidence for the Role of the Lower Crust, Lithosphere, and Asthenosphere in Petrogenesis. *Terrestrial, Atmospheric and Oceanic Sciences*, **22**, 15-40

[39] Wilson, M. (1989) Igneous Petrogenesis a Global Tectonic Approach. Unwin Hyman, London, 466 p. https://doi.org/10.1007/978-1-4020-6788-4

[40] Brian, M. and Carleton, B.M. (1982) Principles of Geochemistry. 4th Edition, John Wiley & Sons, New York, 350

[41] Gunter, F. (1998) Principles and Applications of Geochemistry. 2nd Edition, Prentice-Hall, Inc., Upper Saddle River.

[42] Pearce, J., Harris, N. and Tindle, A. (1984) Trace Element Discrimination Diagram for the Tectonic Interpretation of Granitic Rocks. *Journal of Petrology*, **25**, 956-983. https://doi.org/10.1093/petrology/25.4.956

[43] Shervais, J.W. (1982) Ti-V Plots and the Petrogenesis of Modern and Ophiolitic Lavas. *Earth and Planetary Science Letters*, **59**, 101-118. https://doi.org/10.1016/0012-821X(82)90120-0

[44] Pearce, J.A. and Cann, J.R. (1973) Tectonic Setting of Basic Volcanic Rocks Determined Using Trace Element Analyses. *Earth and Planetary Science Letters*, **19**, 290-300. https://doi.org/10.1016/0012-821X(73)90129-5

[45] Meschede, M. (1986) A Method of Discriminating Between Different Types of Mid-Ocean Ridge Basalts and Continental Tholeiites With the Nb-Zr-Y Diagram. *Chemical Geology*, **56**, 207-218. https://doi.org/10.1016/0009-2541(86)90004-5

[46] Mullen, E.D. (1983) $MnO/TiO_2/P_2O_5$: A Minor Element Discriminant for Basaltic Rocks of Oceanic Environments and Its Implications for Petrogenesis. *Earth and Planetary Science Letters*, **62**, 53-62. https://doi.org/10.1016/0012-821X(83)90070-5

[47] Moghazi, A.K.M. (2003) Geochemistry of a Tertiary Continental Basalt Suite, Red Sea Coastal Plain, Egypt: Petrogenesis and Characteristics of the Mantle Source Region. *Geological Magazine*, **140**, 11-24. https://doi.org/10.1017/S0016756802006994

[48] Zhu, D.C., Pan, G.T., Mo, X.X., Liao, Z.L., Jiang, X.S., Wang, L.Q. and Zhao, Z.D. (2007) Petrogenesis of Volcanic Rocks in the Sangxiu Formation, Central Segment of Tethyan Himalaya: A Probable Example of Plume-lithosphere Interaction. *Journal of Asian Earth Sciences*, **29**, 320-335. https://doi.org/10.1016/j.jseaes.2005.12.004

[49] Al-Hafdh, N.M. and El-Shaafi, A.E.-S.S. (2015) Geochemistry and Petrology of Basic Volcanic Rocks of Jabal Al Haruj Al-Aswad, Libya. *International Journal of Geosciences*, **6**, 109-144. https://doi.org/10.4236/ijg.2015.61008

[50] Fan, Q.-C., Chen, S.-S., Zhao, Y.-W., Zou, H.-B., Li, N. and Sui, J.-L. (2014) Petrogenesis and Evolution of Quaternary Basaltic Rocks from the Wulanhada Area, North China. *Lithos*, **206**-**207**, 289-302. https://doi.org/10.1016/j.lithos.2014.08.007

[51] Lee, H.-Y., Chung, S.-L. and Yang, H.-M. (2016) Late Cenozoic Volcanism in Central Myanmar: Geochemical Characteristics and Geodynamic Significance. *Lithos*, **245**, 174-190. https://doi.org/10.1016/j.lithos.2015.09.018

[52] Niu, Y. and O'Hara, M. (2003) Origin of Ocean Island Basalts: A New Perspective from Petrology, Geochemistry, and Mineral Physics Considerations. *Journal of Geophysical Research*, **108**, 2209. https://doi.org/10.1029/2002JB002048

[53] Wood, D.A., Joron, J.L., Treuil, M., Norry, M.J. and Tannery, J. (1979) Elemental and Sr Isotope Variations in Basic Lavas from Iceland and the Surrounding Ocean Floor. *Contributions to Mineralogy and Petrology*, **70**, 319-339. https://doi.org/10.1007/BF00375360

[54] Bakhsh, R.A. (2015) Pliocene-Quaternary Basalts from Harrat Tufail, Western Saudi Arabia: Recycling of Ancient Oceanic Slabs and Generation of Alkaline Intra-Plate Magma. *Journal of African Earth Sciences*, **112**, 37-54. https://doi.org/10.1016/j.jafrearsci.2015.08.010